Drug Design, Development and Therapy

Dovepress

open access to scientific and medical research

Open Access Full Text Article

ORIGINAL RESEARCH

Transferrin-Modified Mangiferin-Loaded SLNs: Preparation, Characterization, and Application in A549 Lung Cancer Cell

Qi Zhou, Kezhu Hou, Zhiqiang Fu

Department of Thoracic Surgery, Shanghai Shidong Hospital, Shanghai, 200438, People's Republic of China

Correspondence: Kezhu Hou; Zhiqiang Fu, Department of Thoracic Surgery, Shanghai Shidong Hospital, Yangpu District, Shanghai, 200438, People's Republic of China, Email phuang718@163.com; fuzhiqiang1311@163.com

Introduction: Mangiferin is a plant antitumor compound with poor water solubility and low bioavailability. In this study, transferrin-modified mangiferin-loaded solid lipid nanoparticles (Tf-modified MGF-SLNs) were prepared to overcome the above defects.

Methods: Tf-modified MGF-SLNs were prepared by the emulsification-solvent evaporation method. The physicochemical properties of Tf-MGF-SLNs such as particle size, zeta potential and in vitro drug release were investigated. We also demonstrated the effect of Tf-MGF-SLNs in lung cancer.

Results: The mean hydrodynamic diameter of the Tf-MGF-SLNs was 121.8±2.9 nm with a polydispersity index of 0.134±0.03. According to TEM micrographs, Tf-MGF-SLNs are spherical and uniform, and the EE% was found to be 72.5±2.4%. In vitro release, we identified an initial burst effect release, followed by controlled release, in SLNs at both pHs and the Tf-MGF-SLNs drug accumulation release percentages reached over 68% at pH 4.0 and 72% at pH 7.4 in 6 hours, respectively. In vivo studies showed that depending on surface modification, Tf-MGF-SLNs, which suggested that cell internalization was changed and more drugs entered the cells successfully.

Discussion: Tf-MGF-SLNs were highly efficient in suppressing the tumor growth in xenograft tumor model. Sustained release of the drug delivery system and Tf-modified MGF-SLNs played a major role. Tf-MGF-SLNs would be a promising formulation for the treatment of lung cancer.

Keywords: transferrin, mangiferin, SLNs, A549 lung cancer cell

Introduction

Lung cancer (LC) is a highly heterogeneous malignant tumor, accounting for nearly a quarter of the global cancer-related deaths, and nearly 45% of the cases are lung adenocarcinoma (LUAD).[1,2] Due to the lack of early detection techniques and identifiable symptoms, more than 60% of LC patients are diagnosed with local metastasis or advanced stage. For these patients, routine surgery may not be a useful option. Although great progress in treatment strategies has improved the prognosis of some LUAD patients, the overall survival rate within 5 years is still less than 20%.[3] Therefore, it is urgent to further study the new drugs and mechanisms of LUAD.

Mangiferin (MGF) is a xanthone, which exists in different parts of higher plants and mango fruits, such as skin, stem, leaf, skin, kernel and core. It is a promising antioxidant with health-related functions such as antiviral, anti-cancer, antidiabetic, anti-oxidation, anti-aging, immunomodulation, liver protection and analgesia.[4] Isomangiferin and homo-mangiferin account for 10% of the total phenols, and also exist in different parts of mango trees, such as leaves, mango peel and twigs.[5,6] Due to their iron chelating ability in Fenton type reaction, they can prevent the production of hydroxyl radical.[7,8] An in vitro experiment showed that MGF had an effect on cell cycle arrest and induced apoptosis of A549 cells. In addition, some studies have shown that MGF plays a reversal or inhibitory role in lung cancer.[9,10] MGF has poor water solubility and low bioavailability: encapsulation in nanosystems should be a useful tool to enhance their solubility

Received: 23 March 2022
Accepted: 6 May 2022
Published: 8 June 2022

and bioavailability.[11] Based on these premises, the purpose of this work is to develop lipid nanoparticles, namely solid lipid nanoparticles (SLN), loaded with MGF to improve the efficacy.

Receptor-mediated endocytosis is an important mechanism for targeting and delivering chemotherapeutic drugs to organs.[12] Many efforts have been made to develop targeted nanoparticles modified with specific ligands. Studies have shown that transferrin receptor is overexpressed in lung cancer cells.[13,14] Therefore, due to the overexpression of transferrin (TF) receptor in a variety of cancers, its role in iron homeostasis, cell proliferation and receptor-mediated endocytosis has been widely used to deliver drugs to cancer cells.[15] Many chemotherapeutic drugs (such as oxaliplatin, adriamycin, 5-fluorouracil, ceramide, DNA and siRNA[16]) have been used to inhibit tumor through Tf-mediated liposomes.

According to the existing literature, there have been some reports on the study of MGF nanoparticles.[17–19] However, there is no systematic report on the basic research of Tf-modified MGF-SLNs in lung cancer. In this study, we hope that the dissolution performance of MGF will be greatly improved by the form of SLNs for the first time. Secondly, in order to further improve the targeted ability of drugs, we modified Tf receptors in the drug delivery system. In the present study, SLNs were formed by emulsification-solvent evaporation method. The physicochemical properties of Tf-MGF-SLNs such as particle size, zeta potential and in vitro drug release were investigated. We also demonstrated the effect of Tf-MGF-SLNs in lung cancer.

Materials and Methods

Materials

MGF was purchased from Jusheng High-Tech Pharmaceutical Co., Ltd. (Hubei, China). 1.2-Distearoyl-*sn*-glycero-3-phosphoethanolamine (DSPE), DSPE-PEG2000-Tf were obtained from Ponsure Biopharma Co., Ltd (Shanghai, China). Egg phosphatidylcholine (EPC) and cholesterol (CHOL) were obtained from Sinopharm Chemical Reagent (Shanghai, China). The A549 cell line was from the American Type Culture Collection (ATCC, Rockefeller, MD, USA). Balb/c Nude mice (male, 6–8 weeks old, 18.0–20.0 g) were obtained from Shanghai Slack Laboratory Animals Co., Ltd. (Shanghai, China). All other reagents and solvents were of analytical grade.

Preparation of Tf-MGF-SLNs

Tf-MGF-SLNs were prepared by the emulsification-solvent evaporation method. First, MGF (10 mg), EPC (125 mg), CHOL (55 mg) and DSPE-PEG2000–Tf (2 mg) were dissolved in 5 mL chloroform–methanol (3:1, v/v). Therefore, chloroform-methanol was removed under N_2 and evaporated in vacuum for at least 2 hours to form a thin lipid membrane. Add 5 mL of phosphate buffered saline (PBS, pH 7.4, containing poloxamer 407 0.5% w/w) to the hydrated lipid. The liposome suspension was passed through a microfluidic controller for 10 turns at 22,000 bar and then extruded through a polycarbonate membrane with a gradually decreasing pore size (200 and 100 nm) (ten times). Finally, Tf-MGF-SLNs were freeze-dried into powder with the cryoprotectant of mannitol. In addition, blank solid lipid nanoparticles were prepared in a similar manner without the addition of drugs.

Characterization of Tf-MGF-SLNs

Determination of the Entrapment Efficiency (EE%)

The percentage of entrapment efficiency of the prepared Tf-MGF-SLNs was determined by measuring the concentration of free drugs in the dispersion medium. Free drugs were separated from the formulation of nano lipid dispersion by ultracentrifugation. Here, the nano lipid dispersion was centrifuged at 14000rpm for 90 min by using Remi cooling centrifuge. The transparent supernatant of the resulting solution was appropriately diluted with phosphate buffer with pH 5.5 and analyzed by HPLC.

The EE% is calculated from Equation (1).[20]

$$EE\,\% = [(W\ \text{initial drug} - W\ \text{free drug})/W\ \text{initial drug}] \times 100 \quad (1)$$

where "W initial drug" is the mass of initial drug used for the assay and "W free drug" is the mass of free drug detected in the supernatant after centrifugation of the aqueous dispersion.

Particle Size and Zeta Potential Analysis

Particle size and zeta potential were measured for Tf-MGF-SLNs formulae in folded capillary cells using zetasizer. Dilute about 1 mL of each nanodispersions with 10 mL deionized water. Before measuring the size, carry out ultrasonic testing on the sample for 5 minutes.

Transmission Electron Microscope (TEM)

The morphology of Tf-MGF-SLNs dispersion was observed by transmission electron microscope. After dyeing with a drop of 2% w/w phosphotungstic acid aqueous solution, a drop of diluted sample was placed on the surface of carbon coated copper grid. After that, let the sample dry for 10 minutes for examination.

Differential Scanning Calorimetry (DSC) and X-Ray Diffraction (XRD)

DSC analysis was performed by DSC8000 differential scanning calorimeter (Mettler-Toledo International Inc, USA). The accurately weighed samples were placed in an aluminum plate and sealed with a cover. Al_2O_3 was used as the reference material. During the scanning process, a heating rate of 5°C/min was applied with the temperature range from 40°C to 260°C. XRD patterns were obtained at room temperature using a very high-resolution Cu-Kα radiation diffraction system operating at a voltage of 40 kV and current of 30 mA. MS were analyzed in the 2θ angle range of 0–80°.

Stability Studies

The Tf-MGF-SLNs were preserved as lyophilized powder for stability study, and the stability of recombinant lyophilized preparation was studied. The medium used for recombination was phosphate buffered saline with pH 7.4. The stability study protocol complies with ICH Q1A R2 new drug and product stability study guidelines. The samples were subjected to long-term study under cold storage (5°C±3°C) and accelerated study under 25°C±2°C/60%±5% relative humidity. The samples were extracted at the time points of 0, 1, 3 and 6 months, and various physicochemical parameters such as particle size, zeta potential, drug content and entrapment efficiency were evaluated.

HPLC Condition

MGF concentration was analyzed by HPLC (Shimadzu, Kyoto, Japan). Separation was carried out at 30°C using a reverse-phase C18 column (5 μm, 4.6 mm × 250 mm). The mobile phase consisted of methanol and 2% glacial acetic acid (40:60 v:v). The injection volume was 20 μL and the flow rate was 1 mL/min. During all operations, the column temperature is maintained at 30 °C. UV detection was performed at a wavelength of 318 nm. By using MGF of different concentrations in the range of 0.5–150 μg/mL to draw the calibration curve (y=2615x-1421, R^2=0.9993).

Drug Release Study

The release behaviors of MGF in SLNs were investigated in PBS buffer with a pH value of 4.0 and 7.4. Free MGF, MGF-SLNs (1 mg) and Tf-MGF-SLNs (1 mg) were placed in a dialysis bag with a molecular weight cut-off of 14,000. The dialysis bag was suspended in 18 mL release medium which was incubated at 37°C under constant rotation at 100 rpm. At scheduled time intervals (0, 15, 30, 45, 60, 120, 180, 240 and 360 min), aliquot samples (0.2mL) were withdrawn and assayed for MGF content by HPLC. The volume of dissolution medium was maintained at 18 mL throughout the experiment. The kinetic analyses of the release data were performed using various mathematical models.

Cellular Uptake

A549 cells were grown in RPMI 1640 medium supplemented with 10% (v/v) FBS and 5% antibiotics (100 IU/mL of penicillin G sodium and 100 μg/mL of streptomycin sulfate). Using coumarin-6 as a fluorescent probe, the cellular internalization of free MGF, MGF-SLNs and Tf-MGF-SLNs was observed by confocal microscopy. A549 cells were inoculated in cell culture dishes with an initial density of 1×10^6 cells per dish. The cells were then incubated with coumarin-6-adsorbed free MGF, MGF-SLNs and Tf-MGF-SLNs (equivalent to 0.1 μg/mL of coumarin-6) at 37°C ±0.5°

C for 2 hours. Subsequently, the cells were washed several times with PBS and fixed with 4% paraformaldehyde for 10 minutes. Finally, cells were observed under confocal microscope. To quantitative estimate MGF uptake, cells were seeded at a density of 1×10^5 cells in 24-well plates. When they reached 70–80% confluence, cells were incubated with coumarin-6-adsorbed free MGF, MGF-SLNs and Tf-MGF-SLNs (equivalent to 0.1 μg/mL of coumarin-6). After 2 hours of culture, cells were washed several times with cold PBS. Subsequently, cells were lysed by adding Triton X-100 (0.1%). The fluorescence intensity was measured by a multimode microplate reader at an excitation wavelength of 440 nm and an emission wavelength of 520 nm.

Cytotoxicity Study

The cytotoxicity of blank SLNs, free MGF, MGF-SLNs and Tf-MGF-SLNs was evaluated in A549 cells by MTT assay. Briefly, A549 cells were seeded in a 96-well plate at a density of 1×10^6 cells per well. After 12 hours, different MGF formulations (equivalent to MGF concentrations ranging from 1 μM to 80 μM) were added, and plates were incubated for 24 hours. MGF standard solution was prepared with MGF dissolved in ethanol ranging from 0.01 to 0.8 μM and then 100 times diluted with distilled water. Measurements were taken using a microplate reader.

Antitumor Activity

All animal protocols were approved by the Institutional Animal Care and Use Committee at the hospital of Shidong, and the National Institutes of Health (NIH) guidelines for laboratory animal use and care were followed (No: 2021–09-121). Animals were left to acclimatize for at least 7 days upon arrival from the vendor. Each mouse was injected with the A549 lung cancer cells (1×10^6 cells per mouse) suspended in 100 μL of FBS-free RPMI 1640 medium subcutaneously in the shaved left flank. Six days after the implantation (day 6), mice were randomized into four groups, six mice per group, and injected intravenously via the tail vein with Blank SLNs, free MGF, MGF-SLNs and Tf-MGF-SLNs. The dose of MGF was 10 mg/kg body weight. Injection was repeated on days 9 and 12 post implantation. Tumor sizes were measured using a digital caliper, and tumor volumes were calculated using the following formula:

$$\text{Tumor volume } (mm^3)=[\text{Length}\times\text{Width}\times\text{Width}]\times0.5$$

On day 21, mice were euthanized to harvest tumor tissues, which were weighed, fixed in Zn formalin buffer for immunohistochemistry.

Immunohistochemistry

Formalin fixed tumor tissue was embedded in paraffin, sectioned and stained with anti-CD31 antibody as a marker of angiogenesis (n=3). Then scan the slides and take images using scanscope XT.

Biodistribution Study

A549 lung cancer cells were implanted in mice as mentioned above. Three weeks after tumor implantation, the mice were divided into two groups (n=10); One group was injected with MGF in SLNs through caudal vein (equivalent to MGF dose of 15 mg/kg), and the other group was injected with Tf-MGF-SLNs (equivalent to MGF dose of 15 mg/kg). After 2 or 12 hours, five mice in each group were euthanized to collect tumor, liver, kidney, spleen, heart, lung and blood samples. Organs and tumor tissues were weighed and then stored at −80 °C. The blood sample was mixed with EDTA solution, allowed to stand for about 15 minutes, centrifuged (3300g, 10 minutes, 4 °C) to separate the plasma and stored at −80 °C. MGF was extracted from the samples using acetonitrile–glacial acetic acid (9:1, v:v), and MGF concentrations in the samples were determined using HPLC. 4-Nitrophenol was used as an internal standard.

Statistical Analysis

At least three separate determinants of each result are stated as mean ± standard deviation (S.D.). The GraphPad Prism 9 software was used to calculate the data value. $p < 0.05$ was considered as the statistically significant difference.

Results

Preparation and Characterization

In the current study, after screening different concentrations of solid lipids and surfactants by different preparation methods, Tf-MGF-SLNs was well realized by the improved emulsion solvent evaporation method, because the drug showed high solubility in molten lipids (Figure 1A). The charge interaction between particle and medium is measured as zeta potential parameter. It is considered to be a reference for colloidal stability. As a repulsive surface force, this parameter helps to maintain the separation of dispersed nanoparticles, which helps to improve the stability of the formulation.[21] The zeta potential values of MGF-SLNs and Tf-MGF-SLNs were −13.5 and −18.3 mV, respectively. There were no significant difference in zeta potential between the two SLNs, indicating that Tf modification would not change the colloidal stability. Negative surface charges cause electrostatic repulsion. It can ensure the physical stability of nanoparticles during storage and prevent the formation of aggregates.[22] The average hydrodynamic diameter of Tf-MGF-SLNs was 121.8±2.9 nm and the polydispersity index was 0.134±0.03 (Table 1). Medium-sized nanoparticles of less than 500 nm with a spherical shape have enhanced internalization efficiency in the cell. Spherical particles have the right shape that allows them to attach onto the cells and offer a high volume of the incorporated drug.[23] According to TEM micrographs, MGF-SLNs and Tf-MGF-SLNs are spherical and uniform, indicating that the encapsulation of MGF does not significantly affect the shape of SLNs (Figure 1B and C). The EE% of the prepared Tf-MGF-SLNs was 72.5±2.4%, which is considered to be a good encapsulation efficiency. EE% depends on the composition of the lipid matrix and its crystalline state. It has been reported that in lipid-based drug delivery systems, the binding energy of the drugs with the lipids plays a key role in successful encapsulation of drugs.[24]

The interaction between the drug entity and the excipient in SLNs system was determined by the DSC method. Figure 2A shows the thermal behavior of the pure components and the final preparation (Tf-MGF-SLNs). The MGF peaks appeared clear, demonstrating a sharp characteristic endothermic peak at 246.3°C corresponding to its melting temperature. The DSC thermal behaviors of the blank SLNs and physical mixture were chosen as a reference. The thermogram of Tf-MGF-SLNs showed an endothermic peak at 71.6°C, revealing that MGF existed in SLNs in an uncrystalized from rather than a crystallized one.

The XRD study was carried out with support of DSC to verify the reduction in crystalline nature of MGF in prepared SLNs. The XRD spectrums of MGF and the physical mixture in Figure 2B showed distinct and intense peaks at 2θ scale, indicating the crystalline nature of the drug. The XRD spectrum of blank SLNs was chosen as a reference. In contrast, there was a considerable decline in the intensity of all peaks in the XRD pattern of Tf-MGF-SLNs as shown in Figure 2B. Therefore, it can be revealed that the MGF drug may be in amorphous state in the SLNs formulation.

Stability Studies

The stability studies results showed that after reconstitution the particle size has increased up to 2.5% in Tf-MGF-SLNs. The zeta potential and EE% have not changed much depicting good stability. The EE% of the Tf-MGF-SLNs is reduced by 4% at accelerated condition (25°C ± 2°C/60% ± 5% RH). In long-term studies, the particle size shows increase but

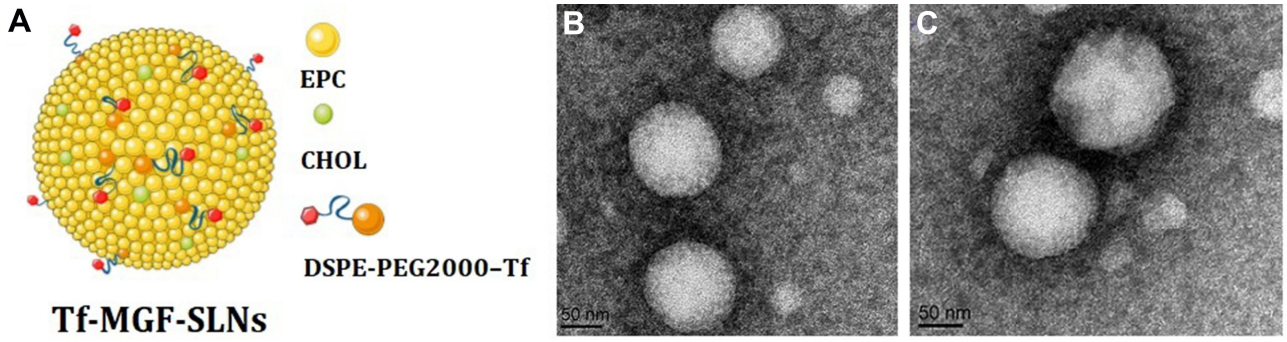

Figure 1 Schematic illustration of Tf-MGF-SLNs (**A**); Transmission electron microscope of MGF-SLNs (**B**); Transmission electron microscope of Tf-MGF-SLNs (**C**).

Table 1 The Characteristics of Different Formulations: Particle Size, Entrapment Efficiency, Polydispersity Index and Zeta Potential. (n=3)

	Particle Size (nm)	Encapsulation Efficiency (%)	Polydispersity Index	Zeta Potential (mV)
MGF-SLNs	117.4±3.3	71.7±4.3	0.142±0.05	−13.5±2.3
Tf-MGF-SLNs	121.8±2.9	72.5±2.4	0.134±0.03	−18.3±1.9

other critical parameters such as EE%, PDI and zeta potential are not much affected in Tf-MGF-SLNs. This ensures good stability of the developed SLNs (Table 2).

Drug Release Study

The in vitro drug release curve of MGF in SLNs was evaluated at pH 7.4 and 5.0 to simulate the physiological pH of blood and the acidic intracellular environment of tumor cells, respectively (Figure 3). Compared with the rapid release of free MGF, the two SLNs groups showed similar sustained-release mode. We identified an initial burst effect release, followed by controlled release, in SLNs at both pHs. At pH 4.0 and pH 7.4, the cumulative release rate of Tf-MGF-SLNs reached more than 72% and 68% within 6 hours, respectively. No differences were observed. Tf-modified SLNs have slightly higher sustained-release effect than unmodified SLNs. Prolonged release indicates that MGF is evenly wrapped throughout the system. The advantage of the extended release system is that the dose and dosage can be reduced by keeping the drug concentration within the treatment window for a long time.[25] This introduction confirms the applicability of SLN as a promising drug carrier. Through analyzing the amount of drug released versus the square root of time, a relatively high correlation coefficient was obtained, indicating that the release followed the Higuchi kinetic model (Q=1.762 t1/2-0.718, r=0.994).

Cellular Uptake

The intracellular internalization of free MGF, MGF-SLNs and Tf-MGF-SLNs in A549 cells was observed by confocal microscope. As shown in Figure 3, strong green fluorescence was observed in the cytoplasmic region after 2 hours of Tf-MGF-SLNs culture. In A549 cells, the internalization rate of Tf-MGF-SLNs was higher than that of other groups. The results showed that, depending on the surface modification, it showed that the internalization of cells changed and more drugs successfully entered the cells. In the quantitative cell uptake study, coumarin-6 in five formulations was quantified by recovering the drug SLNs from cells and measuring its fluorescence. The quantitative results are consistent with the confocal images (Figure 4).

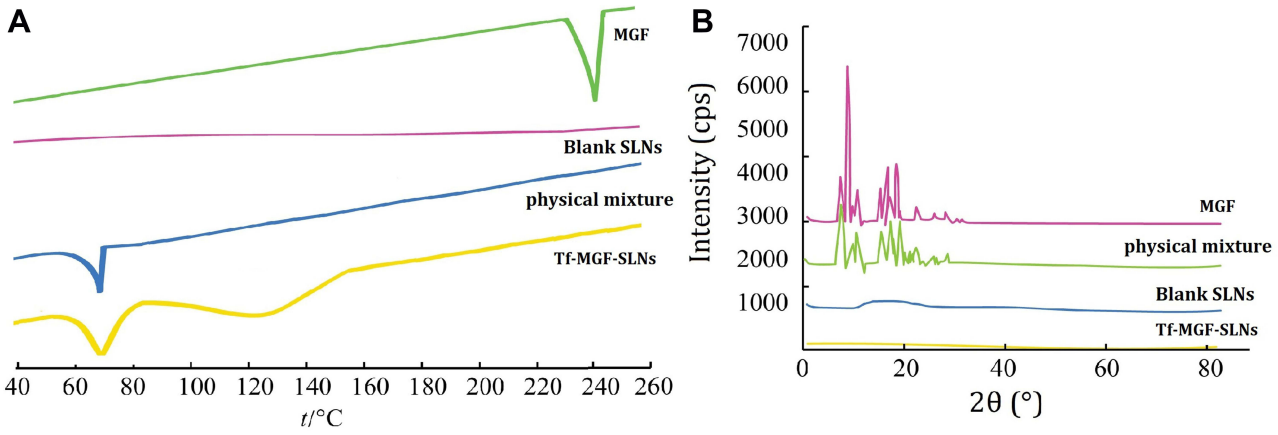

Figure 2 DSC (**A**) and X-ray diffraction spectra (**B**) analyses of the MGF samples.

Table 2 The Stability Studies Results of the Prepared Tf-MGF-SLNs. (n=3)

	Months	Particle Size (nm)	Encapsulation Efficiency (%)	Polydispersity Index	Zeta Potential (mV)
Accelerated studies	0	124.3±3.2	71.6±3.1	0.137±0.04	−18.4±1.6
	1	126.4±4.3	71.5±4.4	0.141±0.03	−19.5±2.7
	3	127.2±4.6	70.9±4.6	0.143±0.05	−18.6±2.3
	6	129.2±3.9	68.8±3.7	0.141±0.05	−19.8±3.2
Long term studies	0	124.3±3.2	71.6±3.1	0.137±0.04	−18.4±1.6
	1	124.2±2.7	71.3±2.5	0.135±0.03	−18.1±1.5
	3	126.3±4.1	71.7±3.2	0.138±0.05	−18.6±2.2
	6	127.1±2.6	70.7±3.1	0.137±0.04	−18.7±1.7

Cytotoxicity Study

The cellular inhibitory effects of different MGF formulations on A549 cells were evaluated by MTT method (Figure 5A). It can be seen that free MGF, MGF-SLNs and Tf-MGF-SLNs showed dose-dependent cytotoxicity to the tested cell lines. Although MGF is a powerful antitumor drug, it can not completely inhibit cell proliferation. Similarly, SLNs binding of MGF did not produce a better effect. On the other hand, Tf aptamer–modified MGF-SLNs significantly reduced cell proliferation and improved treatment efficiency. Surprisingly, Tf-MGF-SLNs showed superior antiproliferative effect on A549 cells. The mechanism may be mediated by Tf aptamer. MGF can be effectively transmitted to tumor tissue, so as to play a therapeutic role. The IC50 values of Tf-MGF-SLNs-treated A549 cells were 7.5 μM, 13.7 μM for MGF-SLNs and 29.1 μM for free MGF (Figure 5B). These data suggested that more drug-loaded Tf-modified SLNs could be internalized into A549 cells which expressed transferrin receptor at higher level, further leading to the significant cytotoxicity by the accumulation of drug in cells.

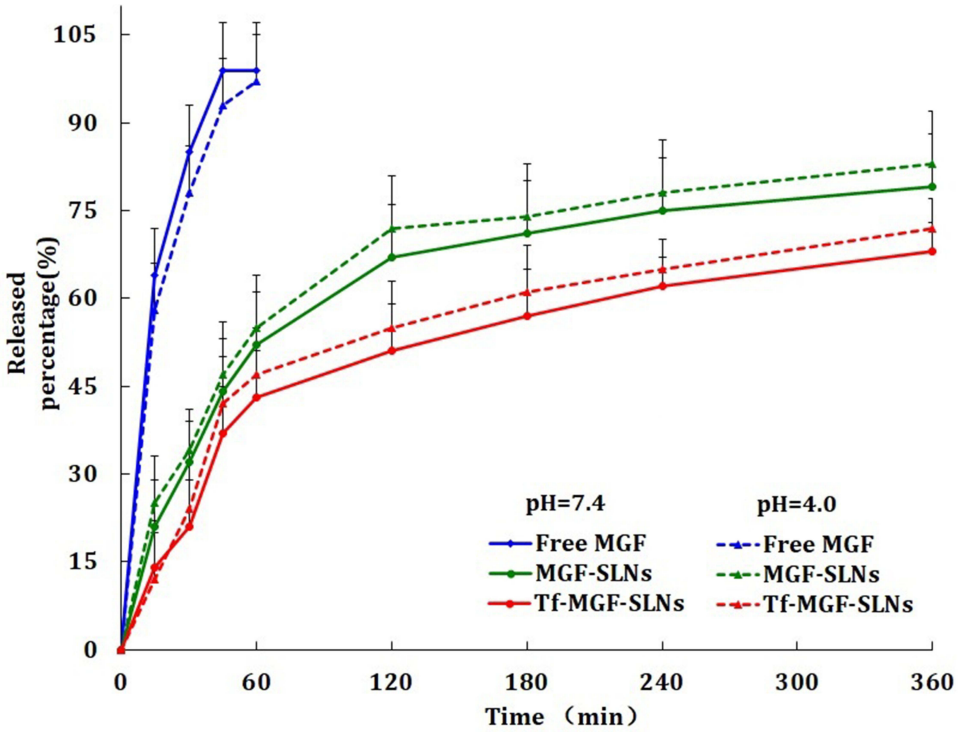

Figure 3 The release profile of MGF in SLNs at the pH values of 7.4 and 5.0 to mimic the physiological pH of blood and the acidic intracellular environment of the tumor cells (n=6).

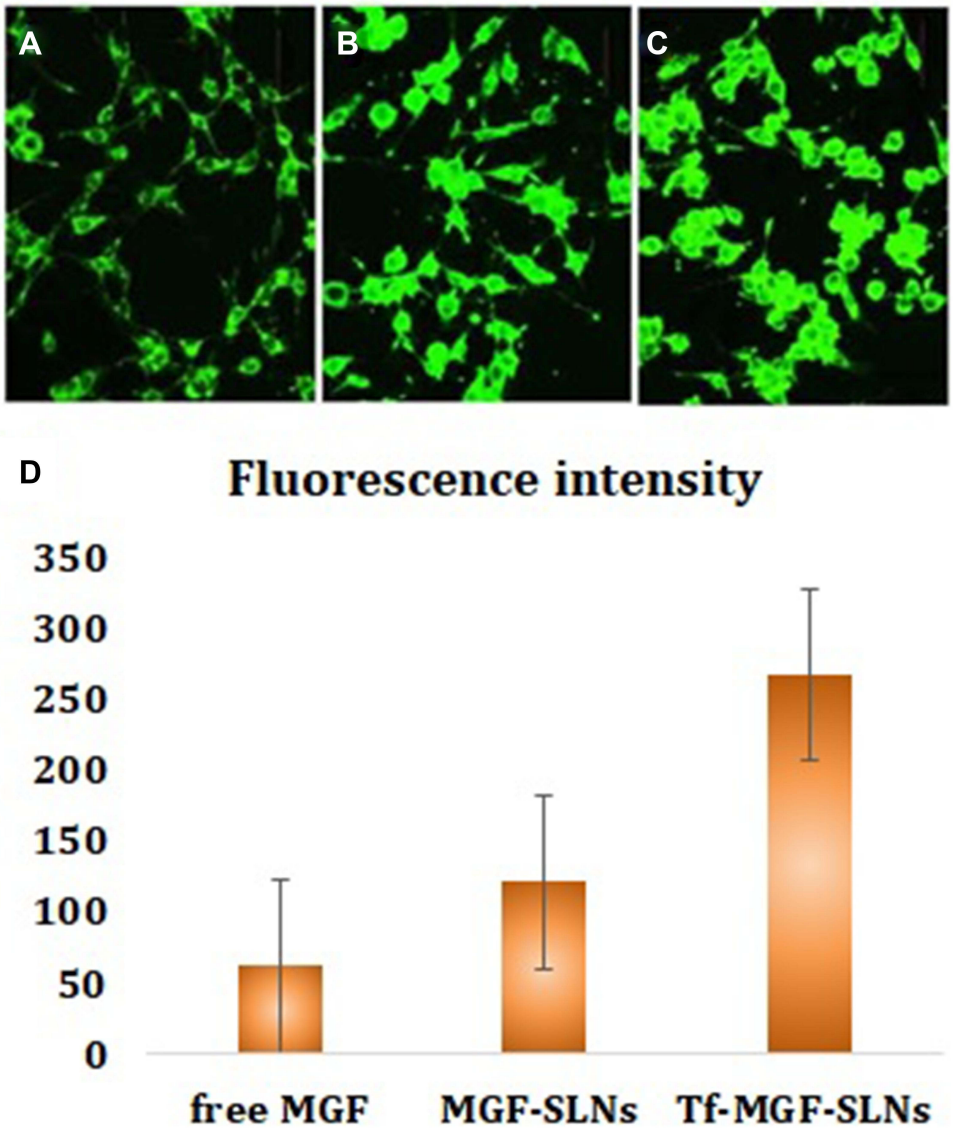

Figure 4 Confocal images of cellular uptake of free MGF (**A**), MGF-SLNs (**B**) and Tf-MGF-SLNs (**C**) by A549 cells. Incubation time was 2 hours. (**D**) was the quantitative results.

Antitumor Activity

The antitumor activity of Tf-MGF-SLNs was evaluated in a pre-established mice A549 lung cancer model. As shown in Figure 6A, both MGF-SLNs and Tf-MGF-SLNs significantly inhibited the growth of mice A549 tumor. However, the Tf-MGF-SLNs were significantly more effective than the MGF-SLNs formulation, starting on day 15. The tumor inhibition effect of free MGF group was the worst, only a little better than that of the control group. The average body weights of mice that were injected with blank SLNs increased slightly (~10%) during the 21 days after tumor cell implantation, while the average body weight of mice that were treated with MGF-SLNs or Tf-MGF-SLNs did not show any significant change (Figure 6B). Finally, at the end of the study, the average tumor weight of mice treated with Tf-MGF-SLNs was also significantly lower than that of other groups (Figure 6C). Anti-CD31 staining (ie, angiogenesis markers) showed that the degree of CD31+ staining was often lower in tumors of mice treated with Tf-MGF-SLNs than in other groups (Figure 7).

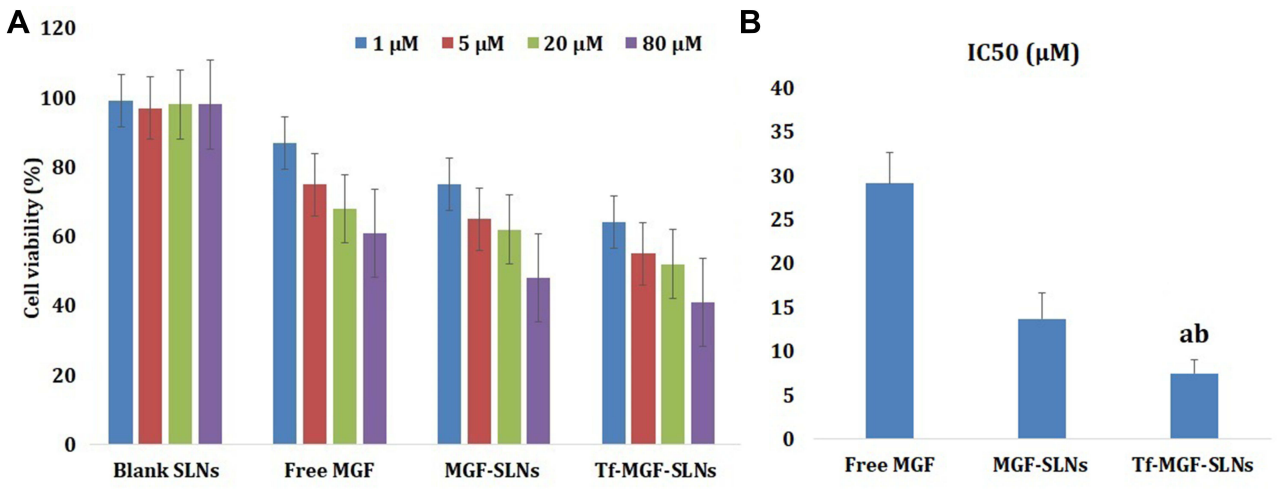

Figure 5 In vitro viability of different MGF formulations in A549 cells. Data represent mean ± SD (n = 3). (**A**) Cell viability cultured with blank SLNs, free MGF, MGF-SLNs and Tf-MGF-SLNs loaded at various concentrations of MGF after 24 h. (**B**) The IC50 values of free MGF, MGF-SLNs and Tf-MGF-SLNs-treated A549 cells. (^{a}p <0.05, Tf-MGF-SLNs vs Blank SLNs, ^{b}p <0.05, Tf-MGF-SLNs vs free MGF, ^{c}p <0.05, Tf-MGF-SLNs vs MGF-SLNs).

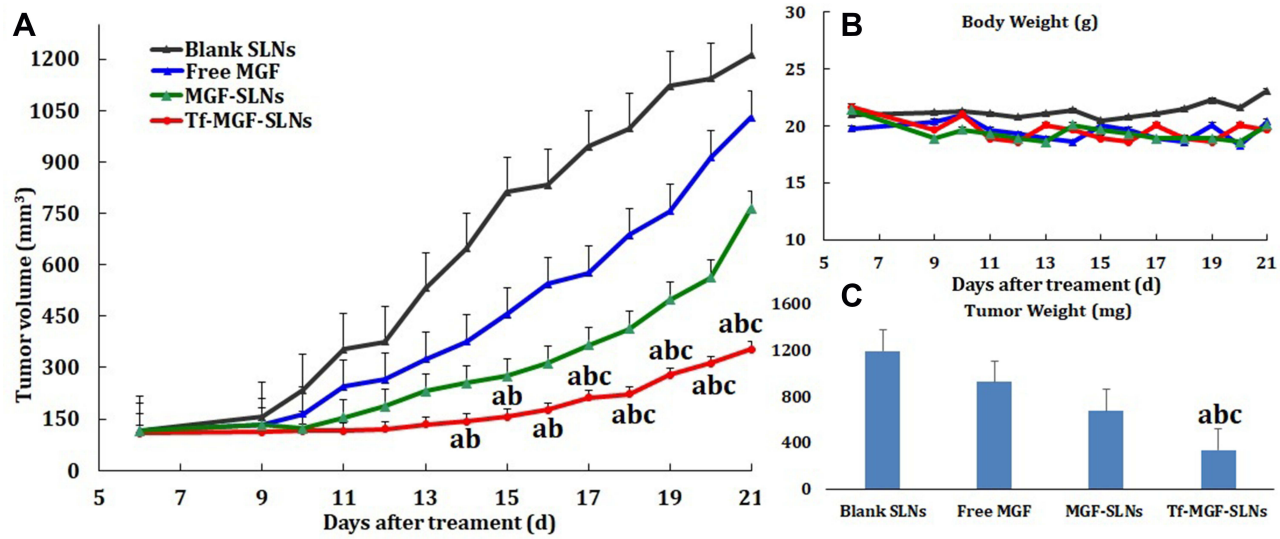

Figure 6 (**A**) The growth curves of A549 tumors in mice. (**B**) The changes in the body weight of A549 tumor-bearing mice. (**C**) The weights of tumors at the end of the study. (^{a}p <0.05, Tf-MGF-SLNs vs Blank SLNs, ^{b}p <0.05, Tf-MGF-SLNs vs free MGF, ^{c}p <0.05, Tf-MGF-SLNs vs MGF-SLNs).

Biodistribution Study

Figure 8 shows the concentration of MGF in tumors and other organs in A549 tumor-bearing mice 2 and 12 h after the mice were injected intravenously with either MGF-SLNs or Tf-MGF-SLNs. The concentration of MGF in tumors in mice that were injected with Tf-MGF-SLNs was about 50% higher than in mice that were injected with the MGF-SLNs formulation, 12 h after the injection ($p < 0.05$). However, the concentration of MGF in the liver, spleen, kidneys, heart, and lungs of mice that were injected with the Tf-MGF-SLNs were lower than in mice that were injected with the MGF-SLNs. Finally, 2 h after intravenous injection, the plasma MGF concentration of mice injected with Tf-MGF-SLNs was about three times that of mice injected with MGF-SLNs.

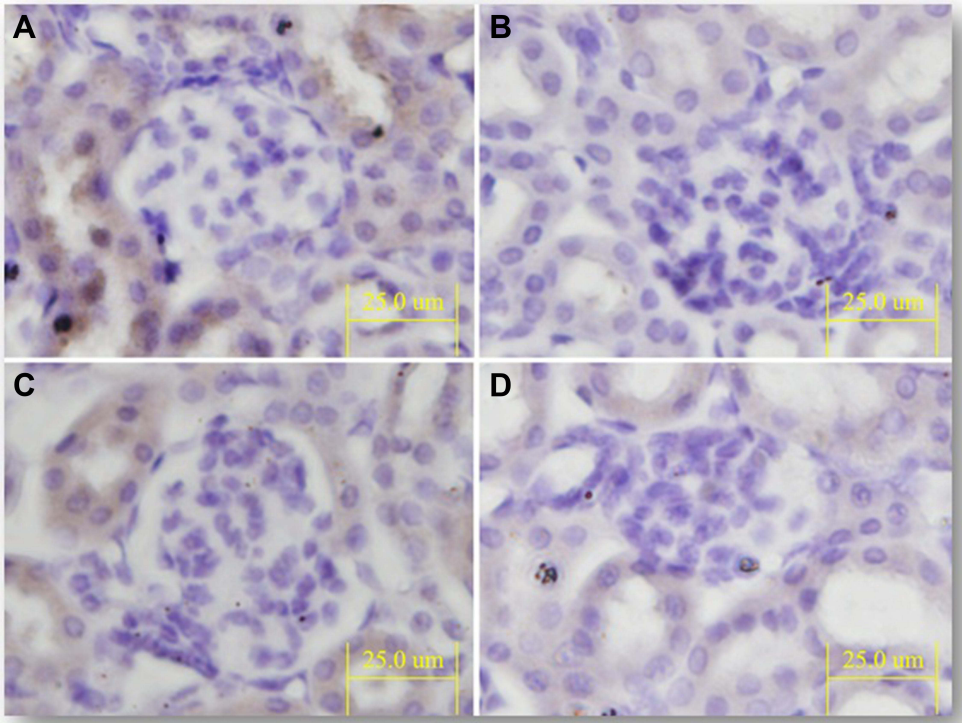

Figure 7 Representative images of tumor tissues after anti-CD31 staining (bar=25 μm). Mice were iv injected with free MGF, MGF-SLNs and Tf-MGF-SLNs at a MGF dose of 10 mg/kg via the tail vein on days 6, 9, and 12 after tumor implantation. Controls included mice that were injected with blank SLNs. (**A**) Blank SLNs; (**B**) free MGF; (**C**) MGF-SLNs; (**D**) Tf-MGF-SLNs.

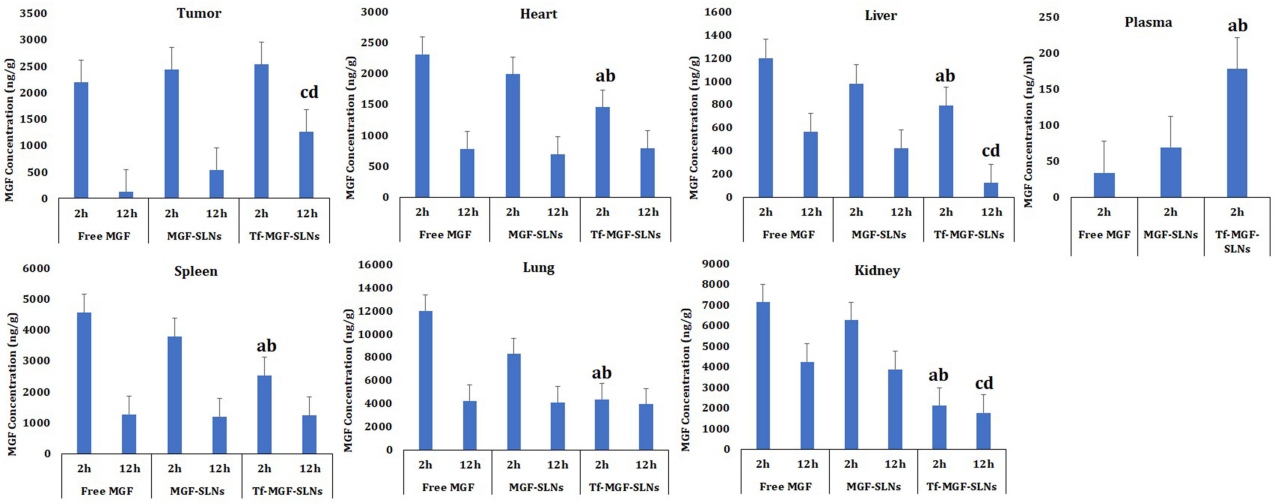

Figure 8 The concentrations of MGF in tumor, heart, liver, spleen, lungs, kidneys and plasma of A549 tumor-bearing mice 2 or 12 h after iv injection of either free MGF, MGF-SLNs or Tf-MGF-SLNs. The dose of MGF was 10 mg/kg. Data shown are mean ± SEM (n=10). (^{a}p <0.05, Tf-MGF-SLNs vs free MGF (2h), ^{b}p <0.05, Tf-MGF-SLNs vs MGF-SLNs (2h), ^{c}p <0.05, Tf-MGF-SLNs vs free MGF (12h), ^{d}p <0.05, Tf-MGF-SLNs vs MGF-SLNs (12h).

Discussion

Many studies have shown that SLNs loaded with chemotherapeutic drugs can be delivered to tumor cells and passively accumulate in tumors in a non-targeted manner by enhancing permeability and retention (EPR) effects. Ideally, if the targeting agent can physically bind to the SLNs surface and deliver the carrier in a targeted manner, it will be a potential method to further enhance the antitumor efficacy. In this study, various key parameters essential for the preparation of Tf-

MGF-SLNs with size of 100–200 nm were optimized by emulsion solvent evaporation method. It has been well documented that particles of <200 nm are more advantageous as nanoparticles of reduced particle size could effectively increase the blood circulation profile of anticancer drugs and thereby avoid the reticuloendothelial system-mediated systemic clearance and passively target the anticancer drug to the tumor tissues.[26]

As related products have been put on the market, the preparation parameters are easier to explore. The purpose of this study is to explore the feasibility of combining Tf with SLNs. Integrin is a kind of cell surface glycoprotein, which mediates cell survival, proliferation and migration through explicit non-covalent interaction with endogenous extracellular matrix (ECM) proteins. They are highly expressed in activated endothelial cells and solid tumor cells, but rarely in resting endothelial cells. Among the members of receptor family, Tf receptor plays an important role in tumor biology, tumor angiogenesis, apoptosis and metastasis. We have developed a new carrier system based on SLNs, which can be modified through Tf to achieve the goal.

The in vitro drug release of MGF in PBS has been studied, and the method of in vitro drug release has been confirmed in the literature. The samples were dispersed in PBS at 37°C and vibration to simulate dynamic conditions in vivo. The results were similar to other nano preparations, showing the consistency of initial burst release in the process of release. The main reason for the burst release is that the drugs on the surface of SLNs are first released into the medium, and then the drug with the core of SLNs. Since Tf modification has no effect on the spatial structure of SLNs, there is no significant difference in the release curve between modified and unmodified SLNs. At the same time, it is relevant to mention that the pH of the cancer microenvironment is acidic, due to hypoxic conditions during uncontrolled proliferation, deficient blood perfusion, and glycolytic cancer cell metabolism. Therefore, to ensure the release of the entrapped drug within the acidic environment and decreased systemic exposure of the drug, we evaluated the release of the drug in two different pH values, which roughly corresponds to the cancer environment and systemic circulation, respectively. We showed that MGF was relatively fast released from the SLNs in an acidic environment, whereas the release pattern at physiological pH was slow.[27] From the results of cell uptake and cell viability, it was also the first time to attempt to verify whether Tf-modified MGF-SLNs could produce a synergistic effect against cancer cells, especially A549 lung cancer cells.[28,29] This also makes the results of this study promising for further clinical application.

Conclusions

In the present study, Tf-modified MGF-SLNs were prepared by the emulsification-solvent evaporation method. The mean hydrodynamic diameter of the Tf-MGF-SLNs was 121.8±2.9 nm with a polydispersity index of 0.134±0.03. According to TEM micrographs, Tf-MGF-SLNs are spherical and uniform and the EE% was found to be 72.5±2.4%. In vitro release, we identified an initial burst effect release, followed by controlled release, in SLNs at both pHs and the Tf-MGF-SLNs drug accumulation release percentages reached over 68% at pH 4.0 and 72% at pH 7.4 in 6 hours, respectively. In vivo studies showed that depending on surface modification, Tf-MGF-SLNs which suggested that cell internalization was changed and more drugs entered the cells successfully. Tf-MGF-SLNs would be a promising formulation for the treatment of lung cancer.

Disclosure

The authors report no conflicts of interest in this work.

References

1. Global Burden of Disease Cancer Collaboration; Fitzmaurice C, Abate D, Abate D, et al. Global, regional, and national cancer incidence, mortality, years of life lost, years lived with disability, and disability-adjusted life-years for 29 cancer groups, 1990 to 2017: a systematic analysis for the global burden of disease study. *JAMA Oncology*. 2019;5(12):1749–1768. doi:10.1001/jamaoncol.2019.2996
2. Siegel RL, Miller KD, Jemal A. Cancer statistics, 2020. *CA Cancer J Clin*. 2020;70(1):7–30. doi:10.3322/caac.21590
3. Lv Y, Huang Z, Lin Y, et al. MiRNA expression patterns are associated with tumor mutational burden in lung adenocarcinoma. *Oncoimmunology*. 2019;8(10):e1629260. doi:10.1080/2162402X.2019.1629260
4. Dar A, Faizi S, Naqvi S, et al. Analgesic and antioxidant activity of mangiferin and its derivatives: the structure activity relationship. *Biol Pharm Bull*. 2005;28(4):596–600. doi:10.1248/bpb.28.596
5. Muruganandan S, Lal J, Gupta PK. Immunotherapeutic effects of mangiferin mediated by the inhibition of oxidative stress to activated lymphocytes, neutrophils and macrophages. *Toxicology*. 2005;215(1–2):57–68. doi:10.1016/j.tox.2005.06.008

6. Sánchez GM, Re L, Giuliani A, Núñez-Sellés AJ, Davison GP, León-Fernández OS. Protective effects of Mangifera indica L. extract, mangiferin and selected antioxidants against TPA-induced biomolecules oxidation and peritoneal macrophage activation in mice. *Pharmacol Res*. 2000;42(6):565–573. doi:10.1006/phrs.2000.0727
7. Matkowski A, Kuś P, Góralska E, Woźniak D. Mangiferin A bioactive xanthonoid, not only from Mango and not just antioxidant. *Mini Rev Med Chem*. 2013;13(3):439–455.
8. Shi W, Deng J, Tong R, et al. Molecular mechanisms underlying mangiferin-induced apoptosis and cell cycle arrest in A549 human lung carcinoma cells. *Mol Med Rep*. 2016;13(4):3423–3432. doi:10.3892/mmr.2016.4947
9. Rajendran P, Rengarajan T, Nishigaki I, Ekambaram G, Sakthisekaran D. Potent chemopreventive effect of mangiferin on lung carcinogenesis in experimental Swiss albino mice. *J Cancer Res Ther*. 2014;10(4):1033–1039. doi:10.4103/0973-1482.137966
10. Lin YS, Tsai KL, Chen JN, Wu CS. Mangiferin inhibits lipopolysaccharide-induced epithelial-mesenchymal transition (EMT) and enhances the expression of tumor suppressor gene PER1 in non-small cell lung cancer cells. *Environ Toxicol*. 2020;35(10):1070–1081. doi:10.1002/tox.22943
11. Gold-Smith F, Fernandez A, Bishop K. Mangiferin and cancer: mechanisms of action. *Nutrients*. 2016;8(7):396. doi:10.3390/nu8070396
12. Fu S, Liang M, Wang Y, et al. Dual-modified novel biomimetic nanocarriers improve targeting and therapeutic efficacy in glioma. *ACS Appl Mater Interfaces*. 2019;11:1841–1854.
13. Riaz MK, Zhang X, Wong KH, et al. Pulmonary delivery of transferrin receptors targeting peptide surface-functionalized liposomes augments the chemotherapeutic effect of quercetin in lung cancer therapy. *Int J Nanomedicine*. 2019;14:2879–2902. doi:10.2147/IJN.S192219
14. Amreddy N, Muralidharan R, Babu A, et al. Tumor-targeted and pH-controlled delivery of doxorubicin using gold nanorods for lung cancer therapy. *Int J Nanomedicine*. 2015;10:6773–6788. doi:10.2147/IJN.S93237
15. Daniels TR, Bernabeu E, Rodriguez JA, et al. The transferrin receptor and the targeted delivery of therapeutic agents against cancer. *Biochim Biophys Acta*. 2012;1820(3):291–317. doi:10.1016/j.bbagen.2011.07.016
16. Koshkaryev A, Piroyan A, Torchilin VP. Increased apoptosis in cancer cells in vitro and in vivo by ceramides in transferrin-modified liposomes. *Cancer Biol Ther*. 2012;13(1):50–60. doi:10.4161/cbt.13.1.18871
17. Razura-Carmona FF, Pérez-Larios A, González-Silva N, et al. Mangiferin-loaded polymeric nanoparticles: optical characterization, effect of Anti-Topoisomerase I, and Cytotoxicity. *Cancers*. 2019;11(12):1965.
18. Khurana RK, Bansal AK, Beg S, et al. Enhancing biopharmaceutical attributes of phospholipid complex-loaded nanostructured lipidic carriers of mangiferin: systematic development, characterization and evaluation. *Int J Pharm*. 2017;518(1–2):289–306. doi:10.1016/j.ijpharm.2016.12.044
19. Md S, Abdullah ST, Alhakamy NA, et al. Ambroxol hydrochloride loaded gastro-retentive nanosuspension gels potentiate anticancer activity in lung cancer (A549) cells. *Gels*. 2021;7(4):243.
20. Agalakshmi S, Ramaswamy SR, Shanmuganathan S. Formulation and evaluation of stimuli sensitive pH triggered in-situ gelling system of Fluconazole in ocular drug delivery. *Int J Pharm Sci Res*. 2014;5:1339–1344.
21. Rahman Z, Zidan AS, Khan MA. Non-destructive methods of characterization of risperidone solid lipid nanoparticles. *Eur J Pharm Biopharm*. 2010;76(1):127–137. doi:10.1016/j.ejpb.2010.05.003
22. Schwarz C, Mehnert W. Solid lipid nanoparticles (SLN) for controlled drug delivery. II. Drug incorporation and physicochemical characterization. *J Microencapsul*. 1999;16:205–213. doi:10.1080/026520499289185
23. Semete B, Booysen LIJ, Kalombo L, et al. In vivo uptake and acute immune response to orally administered chitosan and PEG coated PLGA nanoparticles. *Toxicol Appl Pharmacol*. 2010;249(2):158–165. doi:10.1016/j.taap.2010.09.002
24. Liu Y, Pan J, Feng SS. Nanoparticles of lipid monolayer shell and biodegradable polymer core for controlled release of paclitaxel: effects of surfactants on particles size, characteristics and in vitro performance. *Int J Pharm*. 2010;395:243–250. doi:10.1016/j.ijpharm.2010.05.008
25. Qureshi OS, Kim HS, Zeb A, et al. Sustained release docetaxel-incorporated lipid nanoparticles with improved pharmacokinetics for oral and parenteral administration. *J Microencapsul*. 2017;34:250–261. doi:10.1080/02652048.2017.1337247
26. Ahamed M, Akhtar MJ, Khan MAM, Alhadlaq HA. SnO2-doped ZnO/reduced graphene oxide nanocomposites: synthesis, characterization, and improved anticancer activity via oxidative stress pathway. *Int J Nanomedicine*. 2021;16:89–104. doi:10.2147/IJN.S285392
27. Aldawsari HM, Alhakamy NA, Padder R, Husain M, Md S. Preparation and characterization of chitosan coated PLGA nanoparticles of resveratrol: improved stability, antioxidant and apoptotic activities in H1299 lung cancer cells. *Coatings*. 2020;10(5):439. doi:10.3390/coatings10050439
28. Ahamed M, Akhtar MJ, Khan MAM, Alhadlaq HA. A novel green preparation of Ag/RGO nanocomposites with highly effective anticancer performance. *Polymers*. 2021;13(19):3350. doi:10.3390/polym13193350
29. Ahamed M, Akhtar MJ, Khan MAM, et al. ACS facile synthesis of Zn-Doped Bi2O3 nanoparticles and their selective cytotoxicity toward cancer cells. *Omega*. 2021;6(27):17353–17361. doi:10.1021/acsomega.1c01467